Human Molecular Genetics, 2007, Vol. 16, No. 16 ***1972–1985***
doi:10.1093/hmg/ddm144
Advance Access published on June 18, 2007

Disease-associated mutations affect GPR56 protein trafficking and cell surface expression

Zhaohui Jin[1], Ian Tietjen[2], Lihong Bu[1], Liqun Liu-Yesucevitz[1], Shantanu K. Gaur[1], Christopher A. Walsh[2] and Xianhua Piao[1,*]

[1]Division of Newborn Medicine, Department of Medicine, Children's Hospital and Harvard Medical School and [2]Department of Neurology, Howard Hughes Medical Institute, Beth Israel Deaconess Medical Center and Harvard Medical School, Boston, MA 02115, USA

Received April 11, 2007; Revised and Accepted June 3, 2007

Bilateral frontoparietal polymicrogyria (BFPP) is a congenital brain malformation resulting in irregularities on the surface of the cortex, where normally convoluted gyri are replaced by numerous (poly) and noticeably smaller (micro) gyri. Individuals with BFPP suffer from epilepsy, mental retardation, language impairment and motor developmental delay. Mutations in the gene-encoding G protein-coupled receptor 56 (GPR56) cause BFPP; however, it remains unclear how these mutations affect GPR56 function. Here, we examine the biochemical properties and protein trafficking of wild-type and mutant GPR56. We demonstrate that GPR56 protein undergoes two major modifications, GPS domain-mediated protein cleavage and N-glycosylation, and that the N-terminal fragment can be released from the cell surface. In contrast to the wild-type protein, disease-associated GPR56 missense mutations in the tip of the N-terminal domain (R38Q, R38W, Y88C and C91S) produce proteins with reduced intracellular trafficking and poor cell surface expression, whereas the two mutations in the GPS domain (C346S and W349S) produce proteins with dramatically impaired cleavage that fail to traffic beyond the endoplasmic reticulum. Cell-trafficking impairments are abrogated in part by pharmacological chaperones that can partially rescue mutant GPR56 cell surface expression. These data demonstrate that some BFPP-associated mutations in GPR56 impair trafficking of the mutant protein to the plasma membrane, thus providing insights into how BFPP-associated mutations affect GPR56 function.

INTRODUCTION

Gene-encoding G protein-coupled receptor 56 (GPR56) is an adhesion G protein-coupled receptor (GPCR). Like other members of the adhesion GPCRs (also termed LNB-TM7 or LN-7TM), GPR56 has an unusually long N-terminal extracellular domain containing a high percentage of serine and threonine residues and a GPCR proteolytic site (GPS) domain just before the first transmembrane spanning domain (1–6). The serine and threonine regions can serve as O- and/or N-glycosylation sites, whereas the GPS domain serves as a site for protein cleavage (5,6). GPR56 was originally identified through a degenerate PCR-based approach for secretin-like GPCRs and by differential display of melanoma cell lines with different metastatic potentials (7,8). GPR56 mRNA is selectively expressed in hematopoietic stem cells and neural progenitors, suggesting a role in multipotent cell identity and tissue development (9). In the developing mouse brain, GPR56 mRNA is detected in the embryonic ventricular zone, a region rich in neuronal progenitor cells (10).

Using positional cloning, we recently demonstrated that GPR56 is required for proper development of the human cerebral cortex, as loss-of-function mutations in GPR56 cause a specific human brain malformation known as bilateral frontoparietal polymicrogyria (BFPP) (10). Individuals with BFPP suffer from severe epilepsy, mental retardation, language impairment and motor developmental delay. A total of 11 distinct GPR56 mutations have been reported in BFPP patients, including one deletion, two splicing and eight missense

*To whom correspondence should be addressed at: Division of Newborn Medicine, Department of Medicine, Children's Hospital and Harvard Medical School, 300 Longwood Avenue, Boston, MA 02115, USA. Tel: +1 6179192357; Fax: +1 6177300260; Email: xianhua.piao@childrens.harvard.edu/

mutations (11). Four of the eight missense mutations (R38Q, R38W, Y88C and C91S) are located at the tip of GPR56 N-terminus, two (C346S and W349S) in the GPS domain and two (R565W and L640R) in the transmembrane domain. The deletion mutation, splicing mutations and all missense mutations except one give rise to an indistinguishable BFPP phenotype, suggesting that they all are probably null mutations (10,11). However, the C346S mutation causes a more severe phenotype characterized by an excessively small cerebral cortex called microcephaly, in addition to BFPP (10,11).

Here, we show that GPR56 undergoes two modifications, a GPS-mediated proteolytic cleavage and N-linked glycosylation. The missense mutations at the N-terminal fragment of GPR56 produce proteins that are not trafficked properly to the plasma membrane or secreted. Instead, the majority of mutant proteins are retained in the endoplasmic reticulum (ER) and/or Golgi; however, these effects can be partially reversed by pharmacological chaperones. Our results provide a detailed analysis of the biochemical modifications of GPR56 and address how BFPP-causing missense mutations impair GPR56 protein trafficking and cell surface expression, resulting in a devastating human brain malformation.

RESULTS

BFPP-causing mutations in the GPS domain of GPR56 abolish proteolytic cleavage

GPR56 was shown previously to undergo GPS-mediated proteolytic process resulting in an N-terminal fragment and a C-terminal fragment (12). To characterize the effects of BFPP-associated mutations on GPR56 function, we used site-directed mutagenesis to generate N-terminally VSVG-tagged and C-terminally His-tagged GPR56 and VSVG/His-GPR56 constructs containing R38Q, R38W, Y88C, C91S, C346S, W349S, R565W or L640R point mutation (Fig. 1A). HEK293T cells were transiently transfected with VSVG/His-tagged wild-type or mutant GPR56, and cell lysates were analyzed for cleavage products. In cells that express the wild-type GPR56, western blot analysis with anti-VSVG antibody following SDS–PAGE revealed a predominant band around 60 kDa, in addition to a ladder of higher molecular weight protein bands ranging ~80 kDa (Fig. 1B). The 60 kDa band is larger than the predicted size for the N-terminal fragment of GPR56 ($GPR56^N$), which could reflect modifications such as N- and O-linked glycosylations as often observed in adhesion GPCRs (1,2). Anti-His antibody detected a predominant band of ~22 kDa and a band of ~40 kDa (Fig. 1C). The 22 kDa band is the C-terminal fragment of GPR56 ($GPR56^C$), whereas the 40 kDa band may be a $GPR56^C$ dimer formed by hydrophobic interactions, as often seen in proteins with multiple transmembrane domains (13). The detected $GPR56^C$ is smaller than the predicted size. This phenomenon has been reported previously and could be explained by the highly hydrophobic nature of the C-terminal fragment (12).

In cells expressing R38Q, R38W, Y88C, C91S, R565W and L640R, western blot with VSVG and His antibodies also revealed an N-terminal fragment and a C-terminal fragment, indicating that these mutations do not affect GPS-mediated GPR56 cleavage (Fig. 1B and C). When HEK293T cells were transfected with either C346S or W349S, only the full-size band around 80 kDa was detected by anti-VSVG or anti-His western blot analysis, indicating that C346S and W349S mutations abolish the GPS domain cleavage (Fig. 1B and C). Interestingly, there was a very faint band detected in cells that express W349S in anti-His immunoblot (Fig. 1C, arrow), which corresponds to the cleaved $GPR56^C$.

To identify the subcellular compartment(s) where GPS proteolysis occurs, HEK293T cells were treated with brefeldin A (BFA). BFA is a fungal product that blocks ADP ribosylation factor activation and interferes with anterograde protein trafficking from the ER to the Golgi. At low concentrations, BFA inhibits ER-to-Golgi protein transport, and at high concentrations, it can disrupt the *trans*-Golgi apparatus (14–16). We detected both $GPR56^N$ and $GPR56^C$ following 20 h treatment with various concentrations of BFA, indicating that GPS domain cleavage was not disrupted by BFA treatment and therefore occurs most likely in the ER (Supplementary Material, Fig. S1).

GPR56 is heavily glycosylated

Since the observed size of the $GPR56^N$ is much larger than the predicted unmodified size and GPR56 has multiple potential N-glycosylation sites, we hypothesized that GPR56 is heavily glycosylated. Proteins can be glycosylated at the amide nitrogen in asparagine (Asn) (N-linked) or at the oxygen in serine and threonine side chains (O-linked) (14,17). We first determined the presence of N-linked glycosylation. HEK 293T cells were transiently transfected with VSVG/His-GPR56, and soluble receptors were treated with PNGase F. PNGase F cleaves *N*-glycosyl linkages between Asn and GlcNAc (18) and is therefore one of the most effective reagents to remove virtually all N-linked oligosaccharides from glycoproteins. Following PNGase F treatment, we detected a dramatic band shift for $GPR56^N$: the ~80 kDa ladder together with the 60 kDa band disappeared after PNGase F treatment, resulting in one sharp band remaining at around 40 kDa, the predicted molecular weight of unmodified $GPR56^N$ (Fig. 2A). Similar experiments were performed for the two GPS mutants. PNGase F treatment produced a band shift from 80 to 60 kDa for both C346S and W349S, indicating that uncleaved GPR56 mutant protein was also N-glycosylated (Fig. 2B). In cells expressing R38Q, R38W, Y88C, C91S, R565W and L640R, soluble receptors treated with PNGase F showed the same band shift seen in the wild-type GPR56, indicating that these mutant protein had N-glycosylation modifications similar to the wild-type GPR56 (Supplementary Material, Fig. S2A).

There is no single enzyme that can remove all intact O-linked sugars. Monosaccharides must be sequentially hydrolyzed by a series of exoglycosidases prior to O-glycosidase treatment to remove the Gal-β(1-3)-GalNAc core. To assess the possible presence of O-linked sugars in GPR56, cell lysates were treated with neurominidase (NAMase), which removes sialic acid, and O-glycosidase, which hydrolyzes the common core sugars of O-linked glycans (19,20). SDS–PAGE analysis was then used to identify an electrophoretic mobility shift. The most upper band of the $GPR56^N$ was reduced in size after NAMase treatment compared with the untreated samples

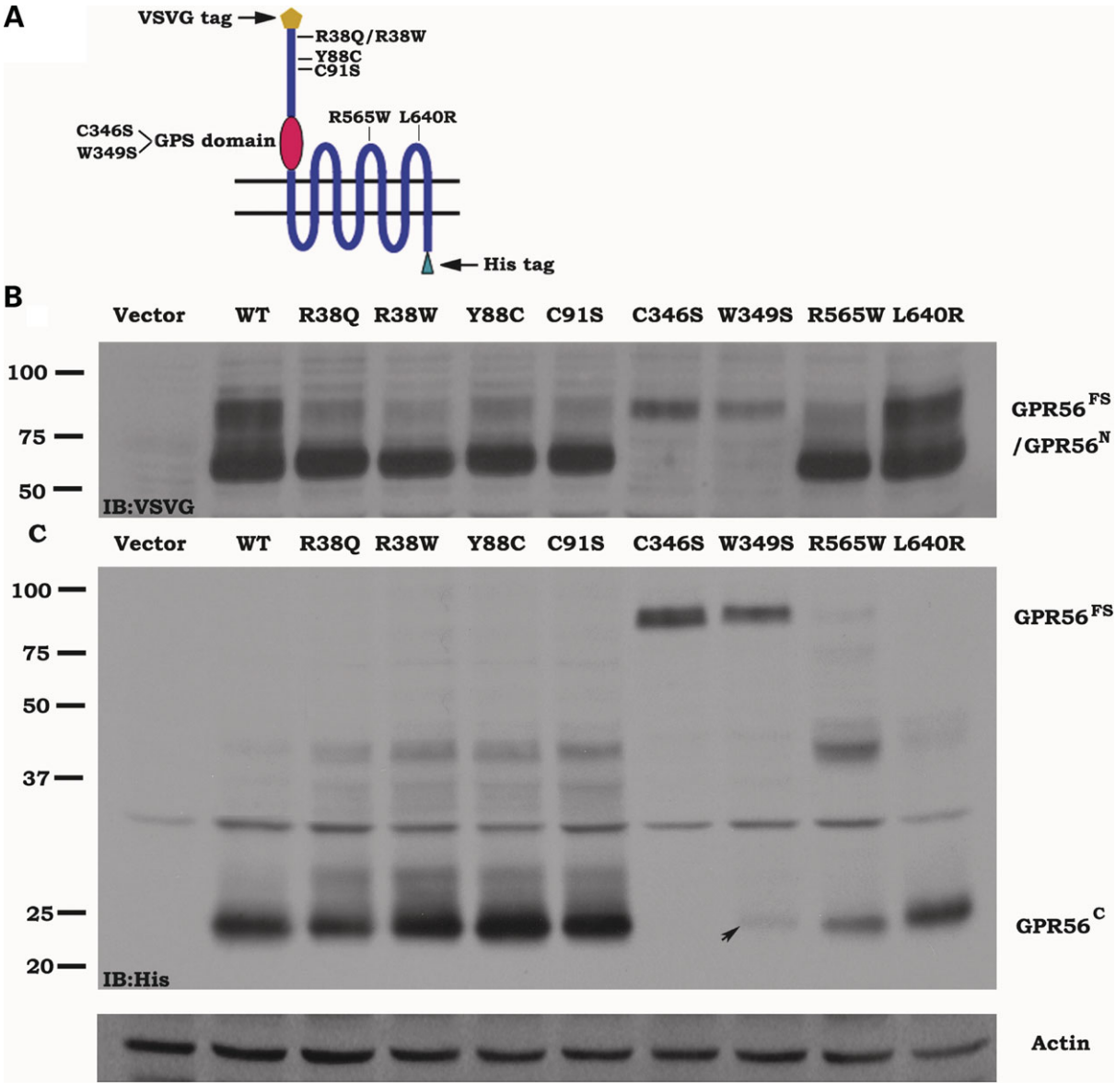

Figure 1. GPS-mediated proteolytic cleavage. (**A**) GPR56 schematic. GPR56 was tagged with VSVG and 6-His at the N- and C-termini, respectively. The positions of the conserved GPS domain are shown. (**B–C**) GPS-mediated protein cleavage. HEK293T cells were transfected with the wild-type VSVG/His-GPR56 (WT) or different GPR56 mutants as indicated. Cells were lysed 48 h after transfection, and soluble receptors were analyzed by SDS–PAGE and western blot using anti-VSVG (B) or anti-His (C) antibodies. The wild-type GPR56, R38Q, R38W, Y88C, C91S, R565W and L640R are cleaved into two distinct fragments. No cleavage products were detected in cells expressing C346S. In cells that express W349S, a faint band corresponding to $GPR56^{C}$ was detected (arrow).

(Fig. 2A). The approximate size difference is 2–3 kDa, consistent with the removal of 5–15 sialic acid moieties. However, there was no difference in apparent size between samples treated with PNGase F alone or with the combination of PNGase F, NAMase and O-glycosidase. These results suggest that GPR56 carries sialic acids that are entirely attached to the N-linked sugar chains. Similar experiments were performed with C346S and W349S mutants, which did not reveal any size shift after NAMase treatment, suggesting that these mutant proteins did not have the sialic acid modification as seen in the wild-type GPR56 (Fig. 2B).

The two GPS mutant proteins migrate as much tighter bands that are not affected by neuraminidase treatment, suggesting that the mutant proteins contain only simple, high mannose oligosaccharides modification. N-glycosylation is initiated in the ER lumen as a high mannosyl oligosaccharide, which is then modified to a complex form in the *cis*-Golgi compartment. We therefore checked whether GPS mutant proteins are stalled in specific intracellular compartments by performing endoglycosidase (endo) H treatment. Endo H cleaves only the high mannose oligosaccharides added in the ER but does not cleave the complex carbohydrate chains synthesized in the Golgi compartment (4,21). GPR56 wild-type protein was partially Endo-H resistant, indicating that it is actively transported to the Golgi apparatus as expected (Fig. 2C). Similar experiments were performed with the eight missense

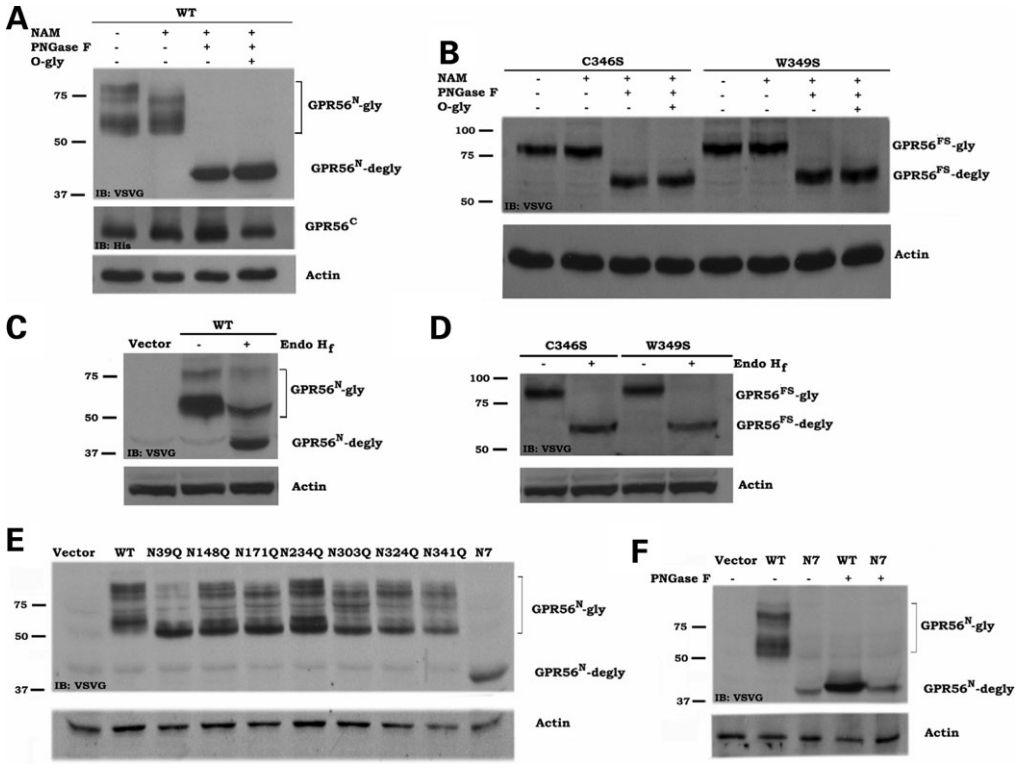

Figure 2. The glycosylated status of GPR56 and its various mutants. (**A** and **B**) Deglycosylation experiment. HEK293T cells were transfected with the wild-type GPR56 (A) or its GPS mutants (B), and cell lysates were treated with various glycosidases as indicated. In the cells that express the wild-type GPR56, both neuraminidase (NAM) and peptide:*N*-glycosidase F (PNGase F) treatment resulted in a band shift for the N-terminal fragment of GPR56 ($GPR56^{N}$), but not *O*-glycosidase (O-glyc). In cells that express C346S or W349S mutant protein, only PNGase F treatment elicited band shift. (**C** and **D**) Endo H_f digestion. HEK293T cells were transfected with wild-type or different mutant GPR56, and cell lysates were treated with or without Endo H_f as indicated. Some wild-type GPR56 was resistant to the Endo H_f treatment, whereas both C346S and W349S were completely sensitive to Endo H_f digestion. (**E**) Identification of N-glycosylation sites. HEK293T cells were transfected with wild-type and various mutants as indicated. Cells were lysed 48 h after transfection and soluble receptors were analyzed by SDS–PAGE and western blot analysis using anti-VSVG antibody. A band shift was detected in all seven mutants where one of the seven N-glycosylation consensus sites was disrupted by the substitution of the Asn to Gln. (**F**) Deglycosylation of $GPR56^{N7}$. HEK 293T cells were transfected with WT or N7 mutant GPR56. Cell lysates were treated in the absence or presence of PNGase F as indicated. There was no band shift seen in cells expressing $GPR56^{N7}$ after PNGase F treatment.

mutants. R38Q, R38W, Y88C, C91S, R565W and L640R revealed comparable result to the wild-type GPR56 (Supplementary Material, Fig. S2B). In contrast, the C346S and W349S mutant proteins were completely sensitive to Endo H digestion, indicating that these proteins contain only high mannose and suggesting that they are not trafficked out of the ER compartment (Fig. 2D). Of note, much reduced levels of the ~80 kDa protein ladders were detected in cells expressing R38Q, R38W, Y88C and C91S in comparison with the wild-type GPR56 (Fig. 1 and S2A). To confirm that this is due to decreased amount of $GPR56^{N}$ that underwent higher order N-glycosylation modification, we performed Endo H treatment on these mutant proteins. Indeed, we detected very little Endo H-resistant ~80 kDa $GPR56^{N}$ in cells expressing R38Q, R38W, Y88C and C91S (Supplementary Material, Fig. S2B).

GPR56 is N-glycosylated at seven sites

We next investigated the extent to which GPR56 is glycosylated. Seven N-linked glycosylation consensus sites (Asn-Xaa-Ser/Thr) are predicted within the N-terminal region of GPR56 at amino acid positions Asn-39, -148, -171, -234, -303 -324 and -341. Using site-directed mutagenesis with primers listed in Supplementary Material, Table S1, we generated a set of GPR56 glycosylation-defective mutants in which only one of the seven glycosylation consensus sites is disrupted by substituting Asn at the consensus site (Asn-Xaa-Ser/Thr) to glutamine (Gln). The mutant receptors were expressed in HEK 293T cells to evaluate each of the seven possible N-glycosylation sites by SDS–PAGE followed by immunoblot with anti-VSVG antibody. A band shift was seen in all seven mutants, indicating that all seven sites are true glycosylation sites for GPR56 (Fig. 2E). We next generated a mutant construct, $GPR56^{N7}$, in which all seven N-glycosylation sites were disrupted. Only a single 40 kDa band was detected in cells expressing $GPR56^{N7}$ by anti-VSVG immunoblot (Fig. 2E). Moreover, PNGase F treatment did not affect the electrophoretic mobility of the N-terminal fragments of the $GPR56^{N7}$ mutant (Fig. 2F). These data further confirm that GPR56 is N-glycosylated at seven sites.

The role of carbohydrate moieties in GPCRs remains unclear although they have been suggested to have variable effects on ligand binding, signal transduction and cell

surface expression. We first tested whether N-glycosylation of GPR56 plays a role in protein trafficking and cell surface expression. SH-SY5Y neuroblastoma cells were transfected with the wild-type GPR56 and its mutant, $GPR56^{N7}$. The cells were then used to perform immunofluorescent staining and biotinylation experiments to evaluate the status of $GPR56^{N7}$ surface expression. There were no VSVG immunoreactivities detected without triton permeabilization, nor were biotinylated N-terminal and C-terminal fragments detected in cells expressing $GPR56^{N7}$ (Supplementary Material, Fig. S3). These results indicate that glycosylation is required for GPR56 protein trafficking and cell surface expression.

BFPP-associated GPR56 mutants affect cell surface expression

To evaluate the effects of GPR56 missense mutations on protein trafficking and cell surface expression in more detail, transfected SH-SY5Y cells were fixed, stained with anti-VSVG antibody and examined by immunofluorescence microscopy. Without triton permeabilization, anti-VSVG antibody detects the surface-expressed VSVG-tagged GPR56. In cells that express the wild-type GPR56 as well as R565W and L640R mutants, anti-VSVG antibody detected abundant signals on the cell surface (Fig. 3Aa), whereas in cells expressing R38Q, R38W, Y88C and C91S, anti-VSVG antibody detected relatively weak signals on the cell surface (Fig. 3Ab–e). In contrast, no VSVG immunoreactivities were detected in cells expressing C346S and W349S (Fig. 3Af and g), despite the presence of comparable expression level of wild-type and mutant GPR56 proteins as evidenced by anti-VSVG antibody staining after triton treatment (Fig. 3Aj–r). In contrast, R565W and L640R transmembrane mutations had robust anti-VSVG antibody staining similar to the wild-type GPR56 (Fig. 3Ah and i). Therefore, N-terminal and GPS missense GPR56 mutant proteins are not properly expressed on the cell surface.

To confirm further that BFPP-associated mutations affect the GPR56 protein cell surface expression, we performed live-cell immunostaining with anti-VSVG antibody. Cells were incubated with anti-VSVG antibody in the culture media for 1 h prior to fixation, triton permeabilization and anti-His immunostaining. We detected VSVG immunoreactivities only in cells expressing the wild-type GPR56, R38Q, R38W, Y88C, C91S, R565W and L640R. No VSVG immunoreactivity was detected in cells expressing C346S or W349S despite the presence of comparable level of the GPR56 protein detected by anti-His antibody among cells expressing the wild-type GPR56 and various mutants (Fig. 3B). Moreover, the percentage of VSVG-positive cells was much lower in cells expressing R38Q, R38W, Y88C and C91S, compared with the cells that express the wild-type GPR56 (Fig. 3C).

To quantify the effect of these mutations on cell surface expression, flow cytometry analysis was used to compare the cell surface expression of GPR56 in cells expressing wild-type and mutant GPR56. SH-SY5Y cells transfected with VSVG/His-tagged wild-type GPR56 and its various mutants were processed with live-cell staining methods. Cell surface-expressed GPR56 was detected by VSVG antibody, and fluorescence signals were analyzed by flow cytometry. These data showed that the overall amount of GPR56 expressed on the cell surface was lower in cells expressing R38Q, R38W, Y88C and C91S (Fig. 3D). The fluorescence signals detected in the wild-type GPR56 (about 58 fluorescent units) were 4–5-fold higher than R38Q, R38W, Y88C and C91S (about 10–15 fluorescent units). In contrast, fluorescence signals detected from R565W and L640R were comparable with the wild-type.

We expected that the cleaved $GPR56^{C}$ was also expressed at the cell surface. We therefore performed biotinylation experiments to confirm the subcellular localization of cleaved $GPR56^{N}$ and $GPR56^{C}$. HEK293T cells transfected with the wild-type or mutant GPR56 were labeled with Sulfo-NHS-Biotin, a membrane impermeable biotinylation agent. The cells were lysed and all biotinylated proteins were isolated by streptavidin affinity chromatography. Using western blot with anti-VSVG or anti-His antibody, we detected both biotinylated $GPR56^{N}$ and $GPR56^{C}$ in the cells that were transfected with the wild-type GPR56 and cells expressing R38Q, R38W, Y88C and C91S, although at much lower levels. In contrast, we did not detect $GPR56^{N}$ or $GPR56^{C}$ in the cells transfected with C346S or W349S (Fig. 4). Therefore, both $GPR56^{N}$ and $GPR56^{C}$ are expressed on the cell surface; however, R38Q, R38W, Y88C and C91S significantly affected the expression efficiency of N-terminal and C-terminal fragments of GPR56 on the cell surface, whereas the non-cleaved full-length C346S and W349S totally abolished the GPR56 cell surface expression. Interestingly, no surface-expressed $GPR56^{C}$ was detected in cells expressing R565W, whereas a disproportionally higher level of $GPR56^{C}$ in comparison with the $GPR56^{N}$ was seen in cells expressing L640R.

Wild-type but not mutant $GPR56^{N}$ is detected in conditioned media

As shown earlier, GPR56 is constitutively cleaved into two subdomains: a large, soluble $GPR56^{N}$ and a membrane-bound, seven-transmembrane $GPR56^{C}$. However, the biological significance of cleaved $GPR56^{N}$ and $GPR56^{C}$ for GPR56 signaling remains unclear. One possibility is that the $GPR56^{N}$ remains non-covalently tethered to the $GPR56^{C}$, and that both fragments continue to function as a single signaling complex. Alternatively, some of the $GPR56^{N}$ could be secreted and function as a reciprocal ligand, as seen in Eph/Ephrin signaling (22–24). To test these possibilities, the conditioned media from transfected cell cultures were subjected to SDS–PAGE and western blot analysis with anti-VSVG antibody. Large amount of glycosylated $GPR56^{N}$ was detected in the conditioned media from cells transfected with the wild-type GPR56 and the two transmembrane mutants (R565W and L640R), but none from cells transfected with the remaining six mutant constructs (Fig. 5). To confirm that the detected $GPR56^{N}$ was not from the cell debris in the conditioned media, the same blot was probed with anti-His antibody. As expected, we did not detect any $GPR56^{C}$ (Fig. 5). Interestingly, the predominant form of $GPR56^{N}$ was heavily glycosylated, in contrast to the cell lysates, where 60 kDa glycosylated $GPR56^{N}$ was the predominant form, suggesting that heavily glycosylated $GPR56^{N}$ is more readily secreted. We anticipated

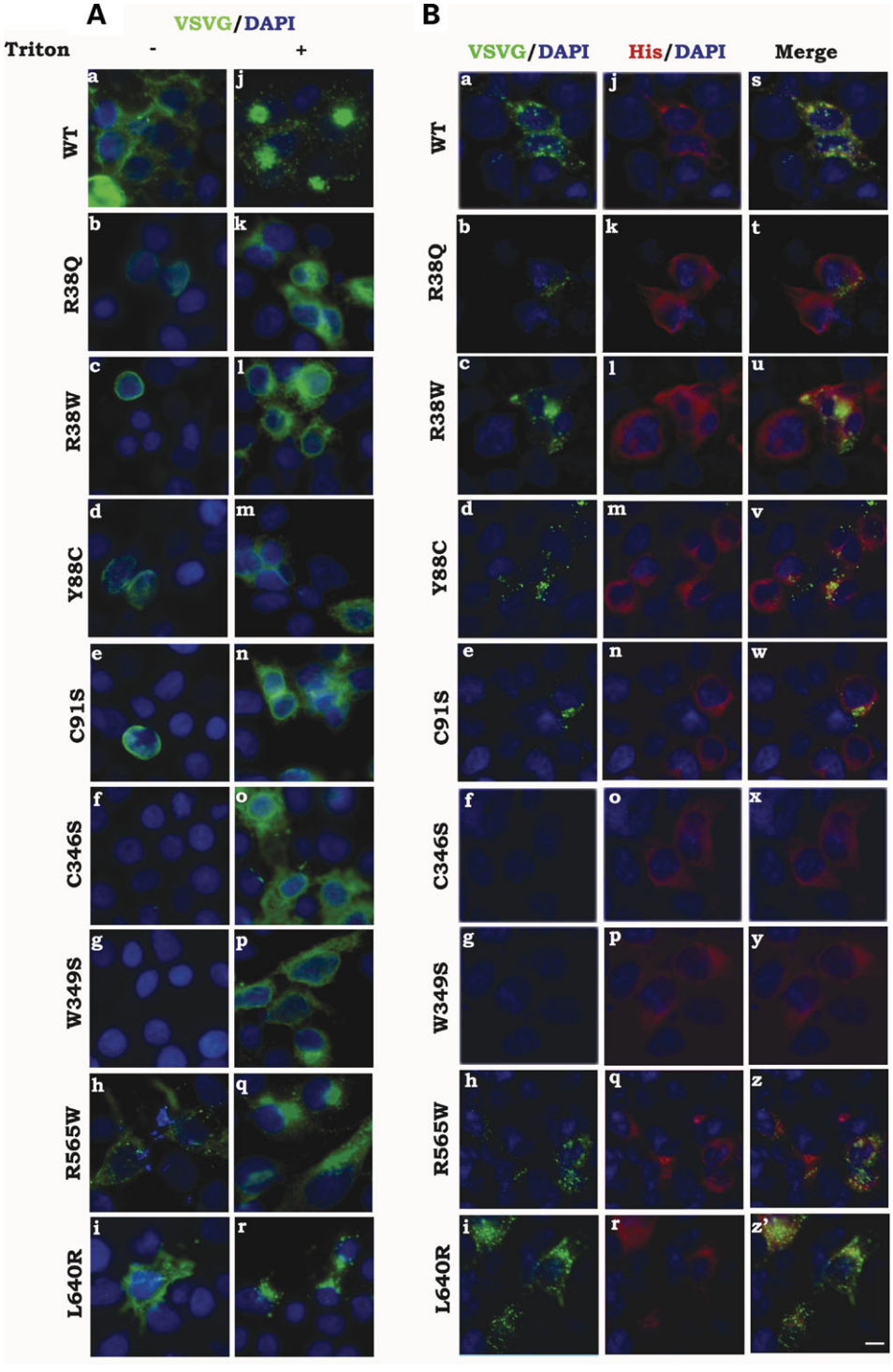

Figure 3. Cell surface expression of the wild-type GPR56 and its various mutants. (**A**) Immunofluorescence analysis on cells treated with or without triton. SH-SY5Y cells transiently transfected with VSVG/His-tagged wild-type GPR56, R38Q, R38W, Y88C, C91S, C346S, W349S, R565W and L640R were fixed and treated without or with 0.1% triton X-100. The cells were stained for GPR56 expression by monoclonal mouse anti-VSVG antibody, and the nuclei were stained with Hoechst 33342. No surface expression was detected in cells expressing C346S or W349S; reduced surface expression was seen in cells expressing R38Q, R28W, Y88C and C91S; normal level of surface expression was seen in cells expressing R565W and L640R. (**B**–**D**) Live-cell immunostaining. Transfected SH-SY5Y cells were first incubated with monoclonal mouse anti-VSVG antibody for 1 h at 37°C in the cultured media. These cells were then fixed, permeabilized and immunostained with anti-His antibody. The nuclei were stained with Hoechst 33342. Again, no surface expression was detected in cells expressing C346S or W349S; reduced surface expression was seen in cells expressing R38Q, R28W, Y88C and C91S; normal level of surface expression was seen in cells expressing R565W and L640R, as evident by fluorescent images (B), percentage of VSVG-positive cells (C) and the mean value of fluorescence (D). Percentage of VSVG-positive cells were counted in the transfected cells (determined by His immunoreactivity). The mean value of fluorescence was determined by the flow cytometry analysis in the population of His-positive cells (determined by His immunoreactivity). Data from three independent experiments are shown. Scale bar 10 μm.

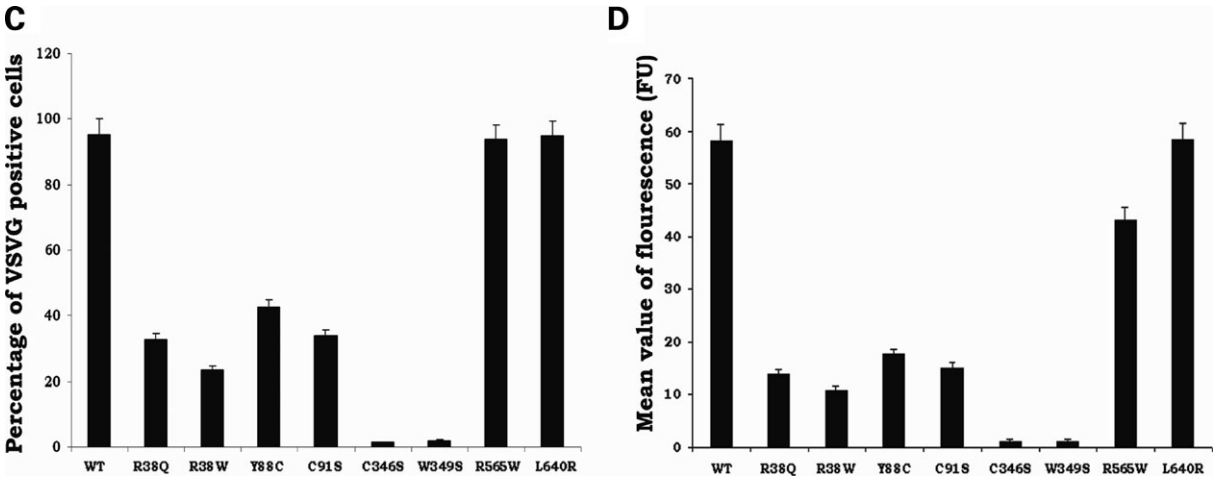

Figure 3. Continued.

that the N-terminal fragments of C346S or W349S would not be secreted into conditioned media because these two mutations completely abolished the GPR56 cell surface expression. However, we also did not detect any secreted $GPR56^N$ in cells expressing R38Q, R38W, Y88C and C91S mutants. This may be due to the low amount of $GPR56^N$ trafficking to the cell surface.

We next performed a series of co-immunoprecipitation experiments with anti-VSVG and anti-His antibodies. As demonstrated in Supplementary Material, Fig. S4A and B, the $GPR56^N$ remains attached to $GPR56^C$ by an SDS- and/or DTT-sensitive linkage. To further confirm the association of $GPR56^N$ and $GPR56^C$ fragments, we performed crosslink experiments using a cell permeable crosslinker [disuccinimidyl suberate(DSS)]. We detected a predominant band around 80 kDa after DSS treatment (Supplementary Material, Fig. S4C). These data demonstrate that some $GPR56^N$ remains associated with $GPR56^C$ following GPS-mediated cleavage.

The lack of cell surface expression of mutant GPR56 is not due to constitutive internalization

The low surface expression of the mutant GPR56 could be due to either constitutively internalization of the mutant protein or failure in the intracellular protein trafficking. Dynamin2 is a GTPase involving in the trafficking of proteins at the cell surface (25). $Dynamin2^{K44A}$ is a dominant negative mutant of dynamin2. When expressed in cells, $dynamin2^{K44A}$ is able to inhibit the internalization of GPCRs (26,27). Thus, $dynamin2^{K44A}$ can be used to determine whether a receptor that is confined to an intracellular compartment is the result of receptor internalization. SH-SY5Y cells were co-transfected with various GPR56 constructs and dynamin2 ($dynamin2^{WT}$/or $dynamin2^{K44A}$). Forty-eight hours after transfection, cells were stained by using the live-cell staining method, and fluorescence signals were detected by flow cytometry. In cells co-expressing the wild-type GPR56 or its two transmembrane

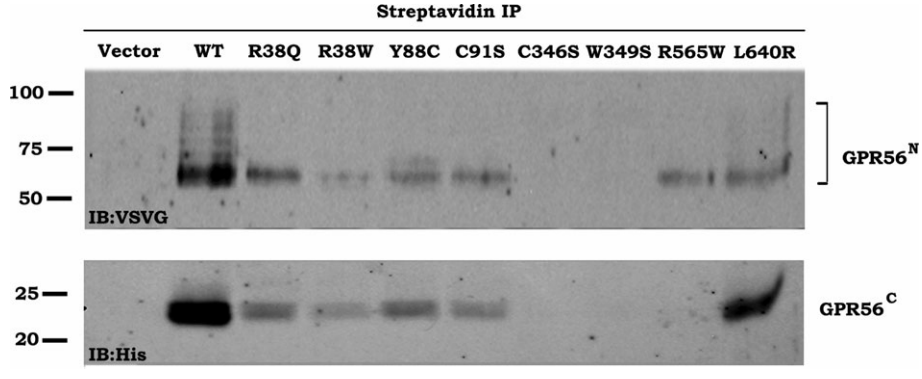

Figure 4. Detection of membrane-expressed GPR56 by biotinylation experiments. Transfected HEK 293T cells were labeled with a membrane-impermeable biotinylation agent and lysed. The biotinylated cell surface proteins were enriched by streptavidin–agarose beads. Streptavidin-purified proteins were then subjected to western blot analysis with anti-VSVG or anti-His antibodies. Both biotinylated $GPR56^N$ and $GPR56^C$ were detected in cells expressing the wild-type GPR56 and cells expressing R38Q, R28W, Y88C and C91S at much lower levels. No $GPR56^N$ and $GPR56^C$ were detected in cells transfected with C346S and W349S. In cells expressing R565W, no $GPR56^C$ was detected, whereas a disproportionately higher level of $GPR56^C$ in comparison with $GPR56^N$ was detected in cells expressing L640R.

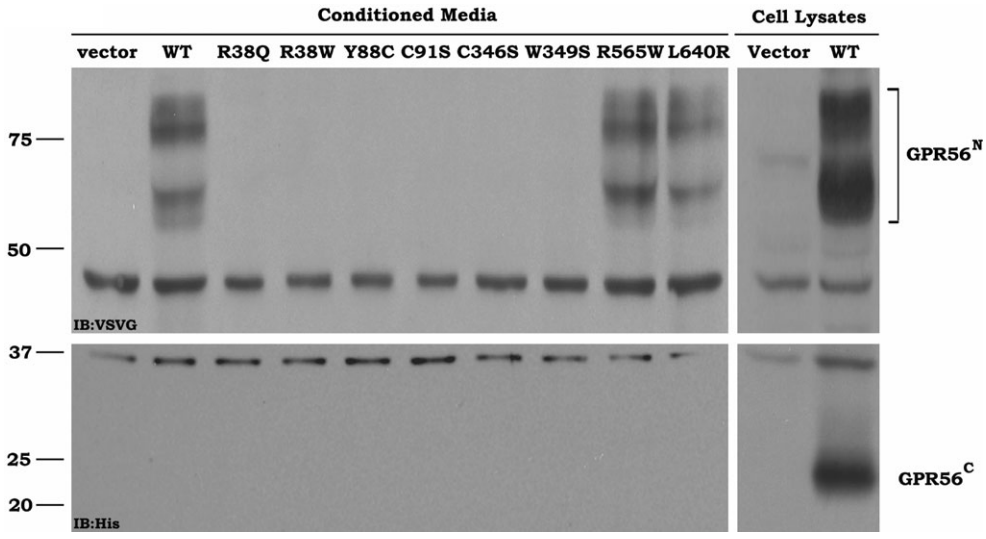

Figure 5. Detection of the secreted GPR56^{N} in the conditioned media. The conditioned media were concentrated, filtered through 0.45 μm pore syringe filter and centrifuged for 10 min at 16 000*g* prior to western blot analysis with VSVG or His antibody, respectively. GPR56^{N} was detected only in the conditioned media harvested from cells expressing the wild-type GPR56, R565W and L640R.

mutants and dynamin2^{K44A}, the cell surface-expressed GPR56 signals were about 2-fold greater than signals from the cells co-transfected with the wild-type GPR56 and dynamin2^{WT}. This result confirmed that dynamin2^{K44A} could inhibit GPR56 internalization. However, in cells expressing R38Q, R38W, Y88C and C91S, the expression of dynamin2^{K44A} did not alter the level of surface-expressed GPR56 (Fig. 6). Therefore, it is unlikely that the low level of cell surface expression of the mutant proteins are caused by receptor internalization, but rather through failure in the receptor intercellular trafficking.

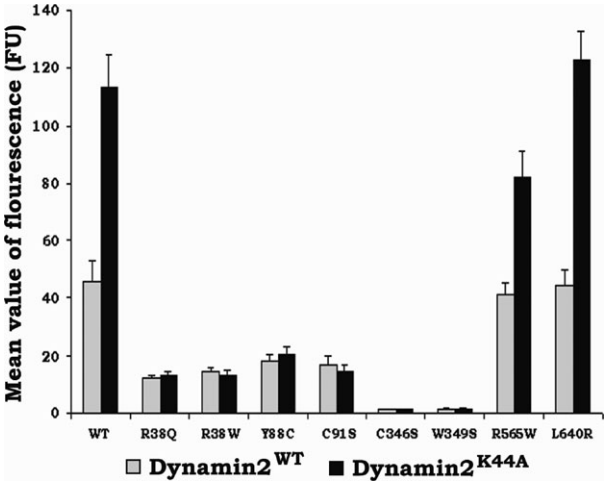

Figure 6. Evaluation of GPR56 receptor internalization. SH-SY5Y cells were co-transfected with various GPR56 constructs and dynamin2 (dynamin2^{WT}/or dynamin2^{K44A}). Transfected SY5Y cells were stained using the live-cell immunostaining, and the mean value of fluorescence was determined by the flow cytometry analysis in the population of His-positive cells (determined by His immunoreactivity). In cells expressing R38Q, R38W, Y88C and C91S, the expression of dynamin2^{K44A} did not alter the level of surface-expressed GPR56. In contrast, R565W and L640R behaved as the wild-type GPR56.

GPR56 mutant proteins are retained in the ER and/or Golgi

To investigate how these BFPP-associated GPR56 mutations affect GPR56 protein trafficking, we performed confocal microscopy studies following double immunostaining with anti-VSVG and anti-calreticulin (ER-associated protein) or anti-His and anti-GM-130 (Golgi complex-associated protein) antibodies (21,28–30). In the cells that express the wild-type GPR56 or the two transmembrane mutants, we detected scattered punctate VSVG signals as well as concentrated signals in the Golgi complex (Fig. 7). In contrast, majorities of R38Q, R38W, Y88C, C91S, C346S and W349S mutant proteins were diffusely distributed within the cells co-localizing with calreticulin immunoreactivity, suggesting that the mutant proteins were retained in the ER (Fig. 7). Moreover, although mutant protein was found in the Golgi of cells expressing R38Q, R38W, Y88C and C91S, no GPR56 mutant proteins co-localized with GM-130 in cells expressing C346S and W349S mutant proteins (Fig. 7). R565W and L640R, on the other hand, had expression patterns that more approximated the wild-type GPR56 subcellular pattern (Fig. 7).

Pharmacological chaperones partially rescue cell surface expression of C346S and W349S mutant proteins

We hypothesized that the N-terminal mutants were trapped in the ER by chaperone proteins due to protein misfolding, as reported in some other disease-causing mutations (31,32). To test this hypothesis, we first analyzed R38Q, R38W, Y88C, C91S, C346S and W349S protein structure using Polyphen (http://genetics.bwh.harvard.edu/cgi-bin/pph/polyphen.cgi) and SIFT (http://blocks.fhcrc.org/sift/SIFT.html) programs, and both programs predicted that these mutations likely induce protein misfolding. We next performed rescue experiments using pharmacological chaperones, thapsigargin and

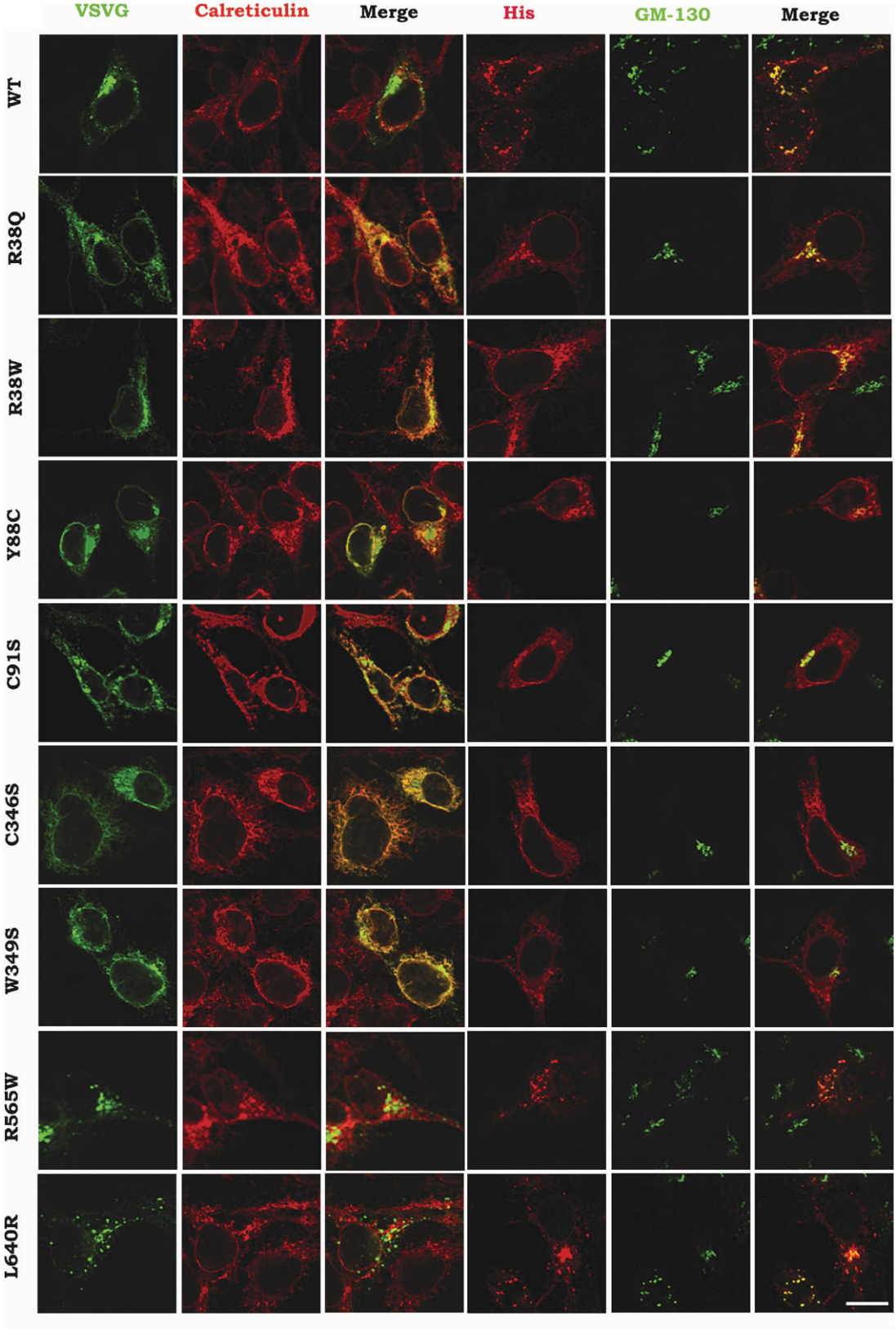

Figure 7. Intracellular retention of GPR56 mutant proteins. Cells expressing the wild-type GPR56 and its various mutant proteins were counterstained with anti-calreticulin (ER) and anti-GM-130 (Golgi complex) antibodies. The wild-type GPR56 is targeted to the plasma membrane but is also found in intracellular compartments including the Golgi apparatus. Most of the BFPP-associated mutants are found mainly in intracellular compartments, notably the ER, where they co-localized in part with calreticulin. The R38Q, R38W, Y88C and C91S mutants are also found in the Golgi apparatus. No major difference was detected in cells expressing R565W and L640W in comparison with the wild-type GPR56. Scale bar 10 μm.

4-phenylbutyrate (4-PBA). Thapsigargin is an ER calcium pump inhibitor that rescues cell surface expression of ER-retained protein by depleting ER calcium stores (33), whereas 4-PBA reduces mRNA and protein levels of the heat-shock protein Hsc70 (34,35). After thapsigargin or 4-PBA treatments, the cell surface expression was rescued at different ranges in cells expressing R38Q, R38W, Y88C, C91S, C346S and W349S (Fig. 8). These results suggested that these mutant proteins are retained in the ER due to protein misfolding and that pharmacological chaperones are able to partially rescue the cell surface expression. The effectiveness of pharmacological chaperones possibly reflects the severity of protein conformational defect (36). The cell surface expression was rescued in much higher percentage of cells expressing R38Q, R38W, Y88C, C91S and W349S than in C346S, suggesting that C346S might induce a much more severe conformational defect.

DISCUSSION

Adhesion GPCRs are a group of signaling molecules that can facilitate cell–cell and cell–matrix interactions (4,5,14, 37–46). GPR56 is a particularly distinct member of the adhesion GPCRs because mutations in GPR56 cause a specific human brain malformation called BFPP (10,11). In the present study, we characterize the biochemical properties of GPR56 and demonstrate how various GPR56 mutations affect GPR56 function. First, we show that GPR56 undergoes proteolytic cleavage at the GPS domain and that GPS mutations (C346S and W349S) abolish GPR56 cleavage. Secondly, we demonstrate that the GPR56 is N-glycosylated at seven sites. Thirdly, the wild-type $GPR56^N$ can be secreted, although there is no detectable $GPR56^N$ in the conditioned media from the six missense mutations in the N-terminal region. Next, the majority of R38Q, R38W, Y88C and C91S mutant proteins are retained in the ER and/or Golgi, whereas no C346S and W349S mutant proteins traffic beyond the ER. Finally, pharmacological chaperones are able to partially rescue the mutant protein cell surface expression.

GPS-mediated protein cleavage is an autocatalytic process (47). The four cysteine and two tryptophan residues in the conserved sequence, $C\text{-}x_2\text{-}W\text{-}x_{6\text{-}16}\text{-}W\text{-}x_4\text{-}C\text{-}x_{11}\text{-}C\text{-}x\text{-}C$, are likely to be essential for proper formation of the catalytic core. The GPS domain was first demonstrated to be an internal

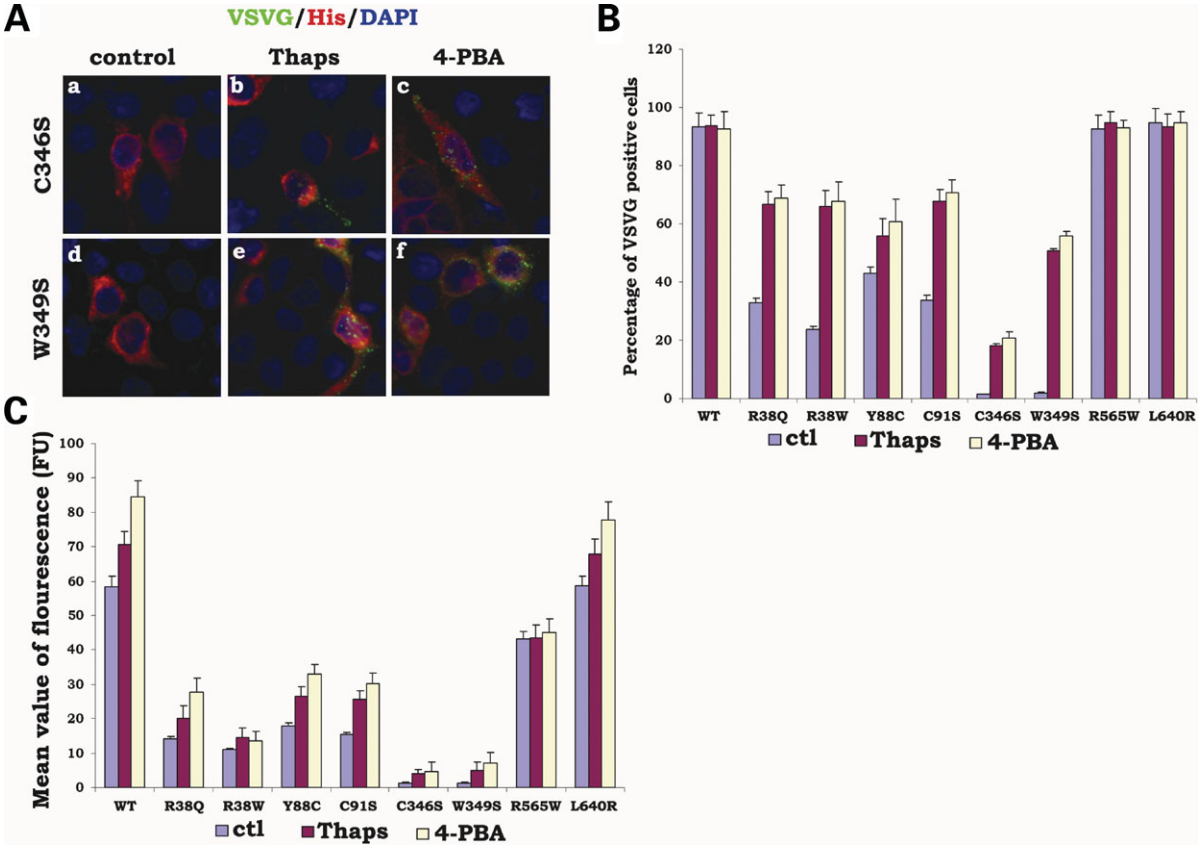

Figure 8. Pharmacological chaperone rescue. Transfected SH-SY5Y cells were first treated with thapsigargin (1 μM) or sodium 4-PBA 1 mM at 37°C for 3 and 24 h, respectively. Monoclonal mouse anti-VSVG antibodies were added to the media for the last hour of the incubation. These cells were then fixed, permeabilized and immunostained with anti-His antibody. Surface expression was rescued by pharmacological chaperone in cells expressing R38Q, R38W, Y88C, C91S, C346S and W349S, as evident by fluorescent images (**A**), percentage of cells rescued (**B**) and the mean value of fluorescence (**C**). One hundred randomly selected cells expressing various GPR56 mutant proteins were analyzed. Cell surface expression of mutant protein was determined by VSVG immunoreactivities. The percentage of cells rescued was calculated by the surface expression of various GPR56 mutants in the transfected cells (determined by His immunoreactivity). The mean value of fluorescence was determined by the flow cytometry analysis in the population of His-positive cells (determined by His immunoreactivity). Data from three independent experiments are shown.

cleavage site in latrophilin and was later found in many other adhesion GPCRs (14,37). Several other proteins outside the adhesion GPCR family, including human polycystic kidney disease protein 1 (PKD-1), and PKDREJ also have the conserved GPS domain (48,49). Here we show that GPR56 is cleaved into an N- and a C-terminal fragment in a manner consistent with GPS-mediated proteolysis, whereas the two mutations in the GPS domain identified in BFPP patients substitute the conserved cysteine or tryptophan residue and thus disrupt this cleavage process. Patients who bear the W349S mutation do not have microcephaly, unlike those with C346S mutation (10). In cells expressing the W349S mutant, we observed leaking cleavage product and better rescue in the cell surface expression. This might explain why patients harboring the W349S mutations have a less severe phenotype than patients bearing the C346S mutations (10,11). Further characterizing the difference between these two mutants at cellular and molecular levels will shed light on the pathogenesis.

Proteins that are destined for secretion or the cell surface are translated in the rough ER and exported to the Golgi, where additional maturation takes place. In the ER, the proteins undergo primary N-glycosylation, where only high mannose oligosaccharides are added. The proteins are then transported to the Golgi complex, where further N-glycosylation and O-glycosylation occur. Protein glycosylation is crucial for promoting proper protein folding, intracellular trafficking, cell surface expression and secretion (17,50). Here, we demonstrate that GPR56 is heavily N-glycosylated and that this carbohydrate modification is important for the GPR56 protein translocation and cell surface expression. The GPR56 N-terminal fragment protein ladders detected in the wild-type represent the complex carbohydrate chains that are added in the Golgi. In contrast, no such modification was detected in the two GPS mutants and very little higher order glycosylation modification occurred for R38Q, R38W, Y88C and C91S (Figs 1 and 2 and S2). This observation is consistent with the finding that both the two GPS mutant proteins and most R38Q, R38W, Y88C and C91S proteins were retained in the ER (Fig. 7).

The N-terminal fragments of several adhesion GPCRs can be non-covalently tethered to their respective membrane-bound C-terminal fragments, which form heterodimers on the cell membrane and function as signaling complexes (37,49,51). Our data show that $GPR56^N$ remains associated with $GPR56^C$. Moreover, our data also showed that some $GPR56^N$ is secreted to the conditioned media, as seen in other adhesion GPCRs (52). It is possible that the $GPR56^N$ could diffuse locally and bind to the reciprocal GPR56 ligand and exert bidirectional signaling, as seen in the cases of Eph receptors and ephrins (22–24). There is no detectable $GPR56^N$ in the conditioned media collected from all six N-terminal missense mutations, indicating that secreted $GPR56^N$ might also be essential for the proper function of GPR56 and cortex development.

Pharmacological chaperones are a group of low-molecular-weight compounds that can reverse the mislocalization and/or aggregation of mutated proteins associated with human diseases (36). The exact mechanisms by which these compounds function are still not fully understood, although it is thought that these pharmacological chaperones may stabilize misfolded protein, prevent protein aggregation or affect the ER chaperone protein activity (36). In this study, we showed that the two pharmacological chaperones, thapsigargin and 4-PBA, can partially rescue the cell surface expression of GPR56 mutant proteins. This finding may open possible strategies to prevent brain malformation in families afflicted with BFPP.

In contrast to the N-terminal and GPS mutations, the two transmembrane mutations did not lead to severe defects in protein trafficking, cell surface expression or N-terminal fragment secretion. Furthermore, the N-terminal and C-terminal fragment interactions were also not affected by the two transmembrane mutations (data not shown). In fact, the only obvious abnormality observed for the two transmembrane mutants was a lack of cell surface-expressed $GPR56^C$ in cells expressing R565W or a disproportionately higher level of $GPR56^C$ in cells expressing L640R (Fig. 4). The two transmembrane mutations may therefore differentially abolish the GPR56 protein function by altering the stability and/or turnover rate of $GPR56^C$. Further investigation of the structural and cell signaling properties of $GPR56^C$ will be required to address this issue.

Although the work described here details the biochemical properties of the GPR56 expression and function, several questions remain unresolved. Notably, the signaling properties of GPR56 are poorly understood. Recently, GPR56 was shown to bind the tissue transglutaminase TG2 (12); however, it remains to be determined whether TG2 functions as a classic ligand for GPR56. Furthermore, GPR56 interacts with the membrane-bound tetraspanin molecules CD9 and CD81 *in vitro*, and CD9/CD81/GPR56 complexes facilitate association with $G\alpha_{q/11}$ and Gβ subunits (53). However, the relationship of GPR56 with CD9, CD81 and downstream signaling targets is not fully studied *in vivo*. Finally, further research is needed to determine the exact role of GPR56, both at the biochemical and at the physiological level, in human cortical development and in human neurological disease.

MATERIALS AND METHODS

Generation of GPR56 expression constructs

All expression constructs were generated using standard molecular biology cloning methods. To generate fusion constructs, cDNA fragments encoding the full-length mouse GPR56 protein were used as a template for PCR. For VSVG/His-GPR56, the primers were forward primer 5′-GGCTCC GGAGAGCCCCCGAGAAGACTTCCGCTTCTG-3′ and reverse primer 5′-CGCCGCGGCCGCTCAATGATGATGATGATG-GATGCGGCTGGAGGAGGTGCTG-3′ (the reverse primer codes for a 6-His tag at the C-terminus of the protein). PCR products were cloned into the *PCR2.1* TOPO system (Invitrogen, Carlsbad, CA), and the DNA fragment was digested with *Bsp*EI and *Not*I and subcloned into VSVG-tagged *pCS2+* vector (gift from Dr Xi He) (54). GPR56 site-directed mutants were made using the QuikChange Site-Directed Mutagenesis Kit (Stratagene, La Jolla, CA) according to the protocols suggested by the manufacturer. Primers used for

the mutagenesis are listed in Supplementary Material, Table S1. All expression constructs were sequenced to confirm their identity.

Cell culture and transfection

HEK293T and SH-SY5Y cells were maintained in Dulbecco's modified Eagle medium with 10% heat-inactivated fetal calf serum and incubated at 37°C with 5% CO_2. Cells were transiently transfected with different expression constructs and LipofectAMINE 2000 (Invitrogen) or FuGENE6 transfection reagent (Roche Diagnostics, Indianapolis, IN) according to the manufacturer's protocol.

Immunoprecipitation, western blot and crosslinking studies

Cells were washed with phosphate-buffered saline (PBS) and resuspended in ice-cold RIPA buffer (1% Nonidet P-40, 50 mM Tris pH 7.6, 120 mM NaCl, 1 mM EDTA) with protease inhibitor cocktail set 1 (Calbiochem, San Diego, CA) and lysed at 4°C for 30 min. The lysates were cleared of insoluble materials by centrifugation at 16 000*g* for 10 min at 4°C. Protein concentration was determined by Bio-Rad protein assay method (Bio-Rad, Hercules, CA) according to the manufacturer's protocol, and equal amount of proteins were used for SDS–PAGE. For immunoprecipitation, cell lysates were pre-cleared with protein A agarose beads at 4°C for 1 h, followed by subsequent incubation with appropriate primary antibody and protein A agarose beads. After extensive washes, the immunopurified proteins were eluted with 8 M urea (50 mM Tris, pH 8.0) and denatured in 2× SDS sample buffer, separated by SDS–PAGE gel and transferred to a nitrocellulose membrane. The membranes were then probed with various antibodies using standard western blot protocols. Crosslink studies were carried out according to the manufacturer's instruction. Briefly, transfected cells were incubated in PBS containing 5 mM DSS (Pierce, Rockford, IL) at room temperate for 30 min with gentle stirring. The reactions were subsequently quenched for 15 min at room temperature by adding 1 M Tris to a final concentration of 20 mM. The cells were then washed, lysed and subjected to immunoprecipitation and western blot analysis as described.

Deglycosylation treatment

HEK-293T cells were transfected with wild-type or different mutant GPR56 constructs. Forty-eight hours after transfection, cells were lysed, and equal amounts of proteins were denatured in denaturing buffer (0.5% SDS, 1% β-mercaptoethanol). Samples were incubated with different combinations of 1 U of PNGase F, 1.0 mU of neuraminidase and/or 0.5 mU of *O*-glycosidase in 50 mM sodium phosphate buffer and 1% NP-40, at 37°C for 4 h prior to SDS–PAGE and western blot analysis.

Biotinylation of cell surface proteins

Biotinylation of cell surface proteins was performed as described (55). Briefly, HEK293T cells were transfected with VSVG/His-tagged wild-type or mutant GPR56 constructs. Twenty-four hours after transfection, cells were washed with ice-cold PBS and incubated with 0.5 mg/ml of Sulfo-NHS-Biotin (Pierce) in PBS for 1 h at 4°C. The cells were subsequently washed extensively in PBS/glycine to remove any unbound biotin prior to lysis with RIPA buffer. Equal amounts of cell lysates were incubated with streptavidin–agarose beads (Sigma, St Louis, MO) for 2 h at 4°C. The beads were then washed three times in RIPA buffer, and the biotinylated proteins were eluted with 8 M urea (in 50 mM Tris, pH 8.0). Samples were further denatured in SDS sample buffer, separated by SDS–PAGE and transferred to a nitrocellulose membrane. The membranes were then probed with various antibodies, using standard western blot protocol.

Detection of secreted N-terminal fragment of GPR56

HEK 293T cells were transiently transfected with VSVG/His-tagged wild-type GPR56 and mutant constructs. Transfected cells were cultured for 72 h, with media changed after the first 24 h. Conditioned media were harvested, centrifuged at 300*g* for 5 min to remove cells and cellular debris, filtered through a 0.45 μm pore syringe filter (Whatman Inc., Clifton, NJ) and concentrated using Centricon Plus-20 spin columns (Millipore, Billerica, MA). The supernatant was further centrifuged at 16 000*g* for 10 min to remove any residual cellular debris. Equal amount of the concentrated conditioned media from different samples were loaded onto SDS–PAGE gel and transferred to a nitrocellulose membrane. The membranes were then probed with rabbit anti-VSVG antibody using standard western blot protocol.

Immunofluorescence staining

SH-SY5Y cells were seeded onto glass coverslips pre-coated with poly-D-lysine (100 μg/ml) 24 h before transfection. Cells were transfected with VSVG/His-tagged wild-type or mutant GPR56 constructs and cultured for another 24 h. The cells on the coverslips were fixed with 4% paraformaldehyde and treated with or without 0.1% triton X-100 for 5 min and blocked with 10% normal goat serum for 1 h, as described (14). Cells were then incubated with proper primary antibodies [rabbit anti-His (1:500; Santa Cruz Biotechnology, Santa Cruz, CA), mouse anti-VSVG (1:200; Roche Applied Science, Indianapolis, IN), rabbit anti-calreticulin (1:500; Affinity BioRegents, Golden, CO) or mouse anti-GM-130 (1:250; BD Bioscience Pharmingen, San Jose, CA)] for 1 h. After rinsing in PBS, samples were incubated with Alexa fluor-488 goat anti-mouse IgG and/or Alexa fluor-546 goat anti-rabbit secondary antibodies for 30 min. Cells were then washed with PBS, and nuclei were stained with Hoechst 33342. Fluorescence was visualized with a Nikon eclipse TE2000-E inverted microscope (40× objective). Representative photographs from cells were obtained with the same exposure setting for wild-type and different mutants. Confocal data were acquired as images of separate channels (Argon ion laser, helium–neon laser and two-photon laser) with a Zeiss LSM 510 confocal microscope (63× oil objective). Identical gain, offset, pinhole and laser settings were used for each

sample. Negative controls for all the immunocytochemistry staining were carried out by omitting primary antibodies (data not shown).

Live-cell staining

Cells seeded on the poly-D-lysine-pretreated coverslips were transfected with VSVG/His-tagged wild-type or mutant GPR56 constructs. Twenty-four hours after transfection, the living cells were first incubated with monoclonal mouse anti-VSVG antibody (1:100) diluted in the culture media for 1 h. These cells were then fixed and treated with 0.1% triton X-100 and blocked with 10% normal goat serum for 1 h. Subsequently, cells were incubated with polyclonal rabbit anti-His antibody for 1 h. After rinsing in PBS, samples were incubated with Alexa fluor-488 goat anti-mouse IgG and Alexa fluor-546 goat anti-rabbit secondary antibodies for 30 min. Cells were then washed with PBS, and nuclei were stained with Hoechst 33342. Fluorescence was visualized with a Nikon eclipse TE2000-E inverted microscope (40× objective). Representative photographs from cells were obtained with the same exposure setting for wild-type and different mutants.

Flow cytometry

SY5Y cells seeded in poly-D-lysine-coated six-well plates were transfected with wild-type GPR56 or different mutants and, in some cases, co-transfected with dynamin2^{WT}/or dynamin2^{K44A} constructs (a kind gift from Dr Mark A. McNiven) (27). Cells were processed for live-cell staining as described earlier. After the last wash, cells were detached from the plate, and cell fluorescence intensity from each well was measured on a FACScan flow cytometer (DAKO).

Pharmacological chaperone treatment

Transfected SY5Y cells were treated with thapsigargin (1 μM, Calbiochem) or sodium4-PBA 1 mM (Sigma) in DMEM culture media at 37°C for 3 or 24 h, respectively. Monoclonal mouse anti-VSVG antibodies were added to the media during the last hour of the incubation. The cells were then processed for live-cell staining as described earlier.

SUPPLEMENTARY MATERIAL

Supplementary Material is available at HMG Online.

ACKNOWLEDGEMENTS

We thank X. He for providing VSVG-tagged *pCS2+* vector, M.A. McNiven for Dyanmin2$^{WT/K44A}$ constructs, Emily Babendreier from the infectious disease division for help with flow cytometry analysis, and the Neurobiology Program Imaging Center for assistance with confocal microscopy. Z.J. was supported by a Flight Attendant Medical Research Institute Young Clinical Scientist Award. I.T. was funded by a Kirschstein-NRSA Individual Postdoctoral Fellowship from the NICHD (F32 HD048035). X.P. was supported by NINDS grant K08 NS045762 and a Child Health Research Grant from the Charles H. Hood Foundation, Inc., Boston, MA. C.A.W. was supported by grant R37 NS35129 from the NINDS and is an investigator of the Howard Hughes Medical Institute.

Conflict of Interest statement. None declared.

REFERENCES

1. Fredriksson, R., Lagerstrom, M.C., Hoglund, P.J. and Schioth, H.B. (2002) Novel human G protein-coupled receptors with long N-terminals containing GPS domains and Ser/Thr-rich regions. *FEBS Lett.*, **531**, 407–414.
2. Fredriksson, R., Gloriam, D.E., Hoglund, P.J., Lagerstrom, M.C. and Schioth, H.B. (2003) There exist at least 30 human G-protein-coupled receptors with long Ser/Thr-rich N-termini. *Biochem. Biophys. Res. Commun.*, **301**, 725–734.
3. Fredriksson, R., Lagerstrom, M.C., Lundin, L.G. and Schioth, H.B. (2003) The G-protein-coupled receptors in the human genome form five main families. Phylogenetic analysis, paralogon groups, and fingerprints. *Mol. Pharmacol.*, **63**, 1256–1272.
4. Krasnoperov, V., Lu, Y., Buryanovsky, L., Neubert, T.A., Ichtchenko, K. and Petrenko, A.G. (2002) Post-translational proteolytic processing of the calcium-independent receptor of alpha-latrotoxin (CIRL), a natural chimera of the cell adhesion protein and the G protein-coupled receptor. Role of the G protein-coupled receptor proteolysis site (GPS) motif. *J. Biol. Chem.*, **277**, 46518–46526.
5. Stacey, M., Lin, H.H., Gordon, S. and McKnight, A.J. (2000) LNB-TM7, a group of seven-transmembrane proteins related to family-B G-protein-coupled receptors. *Trends Biochem. Sci.*, **25**, 284–289.
6. Bjarnadottir, T.K., Fredriksson, R., Hoglund, P.J., Gloriam, D.E., Lagerstrom, M.C. and Schioth, H.B. (2004) The human and mouse repertoire of the adhesion family of G-protein-coupled receptors. *Genomics*, **84**, 23–33.
7. Liu, M., Parker, R.M., Darby, K., Eyre, H.J., Copeland, N.G., Crawford, J., Gilbert, D.J., Sutherland, G.R., Jenkins, N.A. and Herzog, H. (1999) GPR56, a novel secretin-like human G-protein-coupled receptor gene. *Genomics*, **55**, 296–305.
8. Zendman, A.J., Cornelissen, I.M., Weidle, U.H., Ruiter, D.J. and van Muijen, G.N. (1999) TM7XN1, a novel human EGF-TM7-like cDNA, detected with mRNA differential display using human melanoma cell lines with different metastatic potential. *FEBS Lett.*, **446**, 292–298.
9. Terskikh, A.V., Easterday, M.C., Li, L., Hood, L., Kornblum, H.I., Geschwind, D.H. and Weissman, I.L. (2001) From hematopoiesis to neuropoiesis: evidence of overlapping genetic programs. *Proc. Natl Acad. Sci. USA*, **98**, 7934–7939.
10. Piao, X., Hill, R.S., Bodell, A., Chang, B.S., Basel-Vanagaite, L., Straussberg, R., Dobyns, W.B., Qasrawi, B., Winter, R.M., Innes, A.M. *et al.* (2004) G protein-coupled receptor-dependent development of human frontal cortex. *Science*, **303**, 2033–2036.
11. Piao, X., Chang, B.S., Bodell, A., Woods, K., Benzeev, B., Topcu, M., Guerrini, R., Goldberg-Stern, H., Sztriha, L., Dobyns, W.B. *et al.* (2005) Genotype–phenotype analysis of human frontoparietal polymicrogyria syndromes. *Ann. Neurol.*, **58**, 680–687.
12. Xu, L., Begum, S., Hearn, J.D. and Hynes, R.O. (2006) GPR56, an atypical G protein-coupled receptor, binds tissue transglutaminase, TG2, and inhibits melanoma tumor growth and metastasis. *Proc. Natl Acad. Sci. USA*, **103**, 9023–9028.
13. Miedel, M.T., Weixel, K.M., Bruns, J.R., Traub, L.M. and Weisz, O.A. (2006) Posttranslational cleavage and adaptor protein complex-dependent trafficking of mucolipin-1. *J. Biol. Chem.*, **281**, 12751–12759.
14. Volynski, K.E., Silva, J.P., Lelianova, V.G., Atiqur Rahman, M., Hopkins, C. and Ushkaryov, Y.A. (2004) Latrophilin fragments behave as independent proteins that associate and signal on binding of LTX(N4C). *EMBO J.*, **23**, 4423–4433.
15. Ding, W., Albrecht, B., Luo, R., Zhang, W., Stanley, J.R., Newbound, G.C. and Lairmore, M.D. (2001) Endoplasmic reticulum and *cis*-Golgi localization of human T-lymphotropic virus type 1 p12(I): association with calreticulin and calnexin. *J. Virol.*, **75**, 7672–7682.
16. Fujiwara, T., Oda, K., Yokota, S., Takatsuki, A. and Ikehara, Y. (1988) Brefeldin A causes disassembly of the Golgi complex and accumulation

of secretory proteins in the endoplasmic reticulum. *J. Biol. Chem.*, **263**, 18545–18552.
17. Anken, E., Braakman, I. and Craig, E. (2005) Versatility of the endoplasmic reticulum protein folding factory. *Crit. Rev. Biochem. Mol. Biol.*, **40**, 191–228.
18. Maley, F., Trimble, R.B., Tarentino, A.L. and Plummer, T.H., Jr. (1989) Characterization of glycoproteins and their associated oligosaccharides through the use of endoglycosidases. *Anal. Biochem.*, **180**, 195–204.
19. Umemoto, J., Bhavanandan, V.P. and Davidson, E.A. (1977) Purification and properties of an endo-alpha-*N*-acetyl-D-galactosaminidase from *Diplococcus pneumoniae*. *J. Biol. Chem.*, **252**, 8609–8614.
20. Janosi, J.B., Firth, S.M., Bond, J.J., Baxter, R.C. and Delhanty, P.J. (1999) N-Linked glycosylation and sialylation of the acid-labile subunit. Role in complex formation with insulin-like growth factor (IGF)-binding protein-3 and the IGFs. *J. Biol. Chem.*, **274**, 5292–5298.
21. Liewen, H., Meinhold-Heerlein, I., Oliveira, V., Schwarzenbacher, R., Luo, G., Wadle, A., Jung, M., Pfreundschuh, M. and Stenner-Liewen, F. (2005) Characterization of the human GARP (Golgi associated retrograde protein) complex. *Exp. Cell Res.*, **306**, 24–34.
22. Marquardt, T., Shirasaki, R., Ghosh, S., Andrews, S.E., Carter, N., Hunter, T. and Pfaff, S.L. (2005) Coexpressed EphA receptors and ephrin-A ligands mediate opposing actions on growth cone navigation from distinct membrane domains. *Cell*, **121**, 127–139.
23. Davy, A. and Soriano, P. (2005) Ephrin signaling *in vivo*: look both ways. *Dev. Dyn.*, **232**, 1–10.
24. Klein, R. (2005) Axon guidance: opposing EPHects in the growth cone. *Cell*, **121**, 4–6.
25. Conner, S.D. and Schmid, S.L. (2003) Regulated portals of entry into the cell. *Nature*, **422**, 37–44.
26. Fan, J., Perry, S.J., Gao, Y., Schwarz, D.A. and Maki, R.A. (2005) A point mutation in the human melanin concentrating hormone receptor 1 reveals an important domain for cellular trafficking. *Mol. Endocrinol.*, **19**, 2579–2590.
27. Orth, J.D. and McNiven, M.A. (2006) Get off my back! Rapid receptor internalization through circular dorsal ruffles. *Cancer Res.*, **66**, 11094–11096.
28. Liu, L., Done, S.C., Khoshnoodi, J., Bertorello, A., Wartiovaara, J., Berggren, P.O. and Tryggvason, K. (2001) Defective nephrin trafficking caused by missense mutations in the NPHS1 gene: insight into the mechanisms of congenital nephrotic syndrome. *Hum. Mol. Genet.*, **10**, 2637–2644.
29. Ellgaard, L. and Helenius, A. (2003) Quality control in the endoplasmic reticulum. *Nat. Rev. Mol. Cell Biol.*, **4**, 181–191.
30. Jaskolski, F., Coussen, F., Nagarajan, N., Normand, E., Rosenmund, C. and Mulle, C. (2004) Subunit composition and alternative splicing regulate membrane delivery of kainate receptors. *J. Neurosci.*, **24**, 2506–2515.
31. Gregersen, N. (2006) Protein misfolding disorders: pathogenesis and intervention. *J. Inherit. Metab. Dis.*, **29**, 456–470.
32. Gregersen, N., Bross, P., Vang, S. and Christensen, J.H. (2006) Protein misfolding and human disease. *Annu. Rev. Genomics Hum. Genet.*, **7**, 103–124.
33. Egan, M.E., Glockner-Pagel, J., Ambrose, C., Cahill, P.A., Pappoe, L., Balamuth, N., Cho, E., Canny, S., Wagner, C.A., Geibel, J. *et al.* (2002) Calcium-pump inhibitors induce functional surface expression of Delta F508-CFTR protein in cystic fibrosis epithelial cells. *Nat. Med.*, **8**, 485–492.
34. Rubenstein, R.C. and Zeitlin, P.L. (2000) Sodium 4-phenylbutyrate downregulates Hsc70: implications for intracellular trafficking of DeltaF508-CFTR. *Am. J. Physiol. Cell Physiol.*, **278**, C259–C267.
35. Burrows, J.A., Willis, L.K. and Perlmutter, D.H. (2000) Chemical chaperones mediate increased secretion of mutant alpha 1-antitrypsin (alpha 1-AT) Z: a potential pharmacological strategy for prevention of liver injury and emphysema in alpha 1-AT deficiency. *Proc. Natl Acad. Sci. USA*, **97**, 1796–1801.
36. Ulloa-Aguirre, A., Janovick, J.A., Brothers, S.P. and Conn, P.M. (2004) Pharmacologic rescue of conformationally-defective proteins: implications for the treatment of human disease. *Traffic*, **5**, 821–837.
37. Krasnoperov, V.G., Bittner, M.A., Beavis, R., Kuang, Y., Salnikow, K.V., Chepurny, O.G., Little, A.R., Plotnikov, A.N., Wu, D., Holz, R.W. *et al.* (1997) α-Latrotoxin stimulates exocytosis by the interaction with a neuronal G-protein-coupled receptor. *Neuron*, **18**, 925–937.
38. Usui, T., Shima, Y., Shimada, Y., Hirano, S., Burgess, R.W., Schwarz, T.L., Takeichi, M. and Uemura, T. (1999) Flamingo, a seven-pass transmembrane cadherin, regulates planar cell polarity under the control of Frizzled. *Cell*, **98**, 585–595.
39. Curtin, J.A., Quint, E., Tsipouri, V., Arkell, R.M., Cattanach, B., Copp, A.J., Henderson, D.J., Spurr, N., Stanier, P., Fisher, E.M. *et al.* (2003) Mutation of Celsr1 disrupts planar polarity of inner ear hair cells and causes severe neural tube defects in the mouse. *Curr. Biol.*, **13**, 1129–1133.
40. Gao, F.B., Kohwi, M., Brenman, J.E., Jan, L.Y. and Jan, Y.N. (2000) Control of dendritic field formation in *Drosophila*: the roles of flamingo and competition between homologous neurons. *Neuron*, **28**, 91–101.
41. Senti, K.A., Usui, T., Boucke, K., Greber, U., Uemura, T. and Dickson, B.J. (2003) Flamingo regulates R8 axon-axon and axon-target interactions in the *Drosophila* visual system. *Curr. Biol.*, **13**, 828–832.
42. Lelianova, V.G., Davletov, B.A., Sterling, A., Rahman, M.A., Grishin, E.V., Totty, N.F. and Ushkaryov, Y.A. (1997) Alpha-latrotoxin receptor, latrophilin, is a novel member of the secretin family of G protein-coupled receptors. *J. Biol. Chem.*, **272**, 21504–21508.
43. Gray, J.X., Haino, M., Roth, M.J., Maguire, J.E., Jensen, P.N., Yarme, A., Stetler-Stevenson, M.A., Siebenlist, U. and Kelly, K. (1996) CD97 is a processed, seven-transmembrane, heterodimeric receptor associated with inflammation. *J. Immunol.*, **157**, 5438–5447.
44. Nishimori, H., Shiratsuchi, T., Urano, T., Kimura, Y., Kiyono, K., Tatsumi, K., Yoshida, S., Ono, M., Kuwano, M., Nakamura, Y. *et al.* (1997) A novel brain-specific p53-target gene, BAI1, containing thrombospondin type 1 repeats inhibits experimental angiogenesis. *Oncogene*, **15**, 2145–2150.
45. Tissir, F., Bar, I., Jossin, Y., De Backer, O. and Goffinet, A.M. (2005) Protocadherin Celsr3 is crucial in axonal tract development. *Nat. Neurosci.*, **8**, 451–457.
46. Wang, T., Ward, Y., Tian, L., Lake, R., Guedez, L., Stetler-Stevenson, W.G. and Kelly, K. (2005) CD97, an adhesion receptor on inflammatory cells, stimulates angiogenesis through binding integrin counterreceptors on endothelial cells. *Blood*, **105**, 2836–2844.
47. Lin, H.H., Chang, G.W., Davies, J.Q., Stacey, M., Harris, J. and Gordon, S. (2004) Autocatalytic cleavage of the EMR2 receptor occurs at a conserved G protein-coupled receptor proteolytic site motif. *J. Biol. Chem.*, **279**, 31823–31832.
48. Hughes, J., Ward, C.J., Aspinwall, R., Butler, R. and Harris, P.C. (1999) Identification of a human homologue of the sea urchin receptor for egg jelly: a polycystic kidney disease-like protein. *Hum. Mol. Genet.*, **8**, 543–549.
49. Qian, F., Boletta, A., Bhunia, A.K., Xu, H., Liu, L., Ahrabi, A.K., Watnick, T.J., Zhou, F. and Germino, G.G. (2002) Cleavage of polycystin-1 requires the receptor for egg jelly domain and is disrupted by human autosomal-dominant polycystic kidney disease 1-associated mutations. *Proc. Natl Acad. Sci. USA*, **99**, 16981–16986.
50. Ray, K., Clapp, P., Goldsmith, P.K. and Spiegel, A.M. (1998) Identification of the sites of N-linked glycosylation on the human calcium receptor and assessment of their role in cell surface expression and signal transduction. *J. Biol. Chem.*, **273**, 34558–34567.
51. Abe, J., Fukuzawa, T. and Hirose, S. (2002) Cleavage of Ig-Hepta at a 'SEA' module and at a conserved G protein-coupled receptor proteolytic site. *J. Biol. Chem.*, **277**, 23391–23398.
52. Kaur, B., Brat, D.J., Devi, N.S. and Van Meir, E.G. (2005) Vasculostatin, a proteolytic fragment of brain angiogenesis inhibitor 1, is an antiangiogenic and antitumorigenic factor. *Oncogene*, **24**, 3632–3642.
53. Little, K.D., Hemler, M.E. and Stipp, C.S. (2004) Dynamic regulation of a GPCR–tetraspanin–G protein complex on intact cells: central role of CD81 in facilitating GPR56-Galpha q/11 association. *Mol. Biol. Cell*, **15**, 2375–2387.
54. Tamai, K., Zeng, X., Liu, C., Zhang, X., Harada, Y., Chang, Z. and He, X. (2004) A mechanism for Wnt coreceptor activation. *Mol. Cell*, **13**, 149–156.
55. Ohnishi, T., Muroi, M. and Tanamoto, K. (2003) MD-2 is necessary for the toll-like receptor 4 protein to undergo glycosylation essential for its translocation to the cell surface. *Clin. Diagn. Lab Immunol.*, **10**, 405–410.